

Myocardial Recovery in Recent Onset Dilated Cardiomyopathy: Role of CDCP1 and Cardiac Fibrosis

Duan Liu¹, Min Wang¹, Vishakantha Murthy¹, Dennis M. McNamara,† Thanh Thanh L. Nguyen¹, Trudy J. Philips¹, Hridyanshu Vyas¹, Huanyao Gao¹, Jyotan Sahni¹, Randall C. Starling¹, Leslie T. Cooper¹, Michelle K. Skime¹, Anthony Batzler¹, Gregory D. Jenkins, Simona Barlera, Silvana Pileggi¹, Luisa Mestroni¹, Marco Merlo, Gianfranco Sinagra¹, Florence Pinet¹, Jan Krejčí¹, Anna Chaloupka¹, Jordan D. Miller, Pascal de Groote¹, Daniel J. Tschumperlin, Richard M. Weinshilboum, Naveen L. Pereira¹

BACKGROUND: Dilated cardiomyopathy (DCM) is a major cause of heart failure and carries a high mortality rate. Myocardial recovery in DCM-related heart failure patients is highly variable, with some patients having little or no response to standard drug therapy. A genome-wide association study may agnostically identify biomarkers and provide novel insight into the biology of myocardial recovery in DCM.

METHODS: A genome-wide association study for change in left ventricular ejection fraction was performed in 686 White subjects with recent-onset DCM who received standard pharmacotherapy. Genome-wide association study signals were subsequently functionally validated and studied in relevant cellular models to understand molecular mechanisms that may have contributed to the change in left ventricular ejection fraction.

RESULTS: The genome-wide association study identified a highly suggestive locus that mapped to the 5'-flanking region of the *CDCP1* (CUB [complement C1r/C1s, Uegf, and Bmp1] domain containing protein 1) gene (rs6773435; $P=7.12 \times 10^{-7}$). The variant allele was associated with improved cardiac function and decreased *CDCP1* transcription. *CDCP1* expression was significantly upregulated in human cardiac fibroblasts (HCFs) in response to the PDGF (platelet-derived growth factor) signaling, and knockdown of *CDCP1* significantly repressed HCF proliferation and decreased AKT (protein kinase B) phosphorylation. Transcriptomic profiling after *CDCP1* knockdown in HCFs supported the conclusion that *CDCP1* regulates HCF proliferation and mitosis. In addition, *CDCP1* knockdown in HCFs resulted in significantly decreased expression of soluble ST2 (suppression of tumorigenicity-2), a prognostic biomarker for heart failure and inductor of cardiac fibrosis.

CONCLUSIONS: *CDCP1* may play an important role in myocardial recovery in recent-onset DCM and mediates its effect primarily by attenuating cardiac fibrosis.

GRAPHIC ABSTRACT: A [graphic abstract](#) is available for this article.

Key Words: cardiomyopathy, dilated ■ fibrosis ■ genetics ■ genome-wide association study ■ heart failure ■ humans ■ ventricular remodeling

The prevalence of heart failure is projected to increase by 46% from 2012 to 2030 and will affect over 8 million people in the United States by 2030.^{1,2} Targeting the neurohormonal axis has led to improved survival

in heart failure with reduced ejection fraction (HFrEF); however, newer therapies based on this approach have had diminishing returns, and morbidity and mortality for this disease remain high.³ Among patients with HFrEF,

Novelty and Significance

What Is Known?

- Dilated cardiomyopathy (DCM) accounts for 30% to 40% of all cases of heart failure with reduced ejection fraction and is the most common cause of heart transplantation.
- Myocardial recovery in recent-onset DCM after standard pharmacotherapy is highly variable among individuals.
- Cardiac fibrosis is one of the most important predictors of myocardial recovery in DCM.

What New Information Does This Article Contribute?

- We performed a genome-wide association study for changes in left ventricular ejection fraction as the phenotype in 686 patients with recent-onset DCM, which identified a highly suggestive single-nucleotide polymorphism signal mapping to the 5'-flanking region of the *CDCP1* (CUB [complement C1r/C1s, Uegf, and Bmp1] domain containing protein 1) gene.
- The variant allele of the genome-wide association study-identified single-nucleotide polymorphism was significantly associated with decreased *CDCP1* expression and improvement in left ventricular ejection fraction, implicating the possible role of *CDCP1* in myocardial recovery of patients with DCM.
- *CDCP1* knockdown significantly repressed human cardiac fibroblast proliferation stimulated by the PDGF (platelet-derived growth factor) signaling.

To our knowledge, this is the first genome-wide association study for change in left ventricular ejection fraction in recent-onset DCM, which identified a highly suggestive single-nucleotide polymorphism mapping to the 5'-flanking region of the *CDCP1* gene. We also found that genetic variation in/near *CDCP1* was significantly associated with heart failure mortality in the UK Biobank data set. Given that *CDCP1* is highly variably expressed in human fibroblasts among individuals, and because cardiac fibrosis is an important determinant of myocardial recovery in DCM, we pursued its role in cardiac fibrosis. We demonstrated that the single-nucleotide polymorphism variant allele, which was associated with improved left ventricular ejection fraction in the genome-wide association study, resulted in decreased *CDCP1* expression in human cardiac fibroblasts. Of importance, *CDCP1* knockdown significantly decreased human cardiac fibroblast proliferation stimulated by PDGF signaling, a signaling pathway for which activation is known to promote cardiac fibrosis. Transcriptome wide, the gene that was most significantly downregulated in human cardiac fibroblast after *CDCP1* knockdown was *IL1RL1*, which encodes soluble ST2 (suppression of tumorigenicity-2), corroborating the potential beneficial effect of *CDCP1* knockdown on myocardial recovery and fibrosis. Our study raises the possibility of targeting *CDCP1* to decrease cardiac fibrosis with potential for improvement in myocardial function and with implications for novel DCM pharmacotherapy.

Nonstandard Abbreviations and Acronyms

α-SMA	alpha-smooth muscle actin
ACE	angiotensin-converting enzyme
CAR	chimeric antigen receptor
CDCP1	CUB domain containing protein 1
COL1A1	collagen type I alpha 1 chain
COL5A1	collagen type 5 alpha 1 chain
DCM	dilated cardiomyopathy
DEG	differentially expressed gene
ECM	extracellular matrix
FN-1	fibronectin-1
GWAS	genome-wide association study
HCF	human cardiac fibroblast
HFrEF	heart failure with reduced ejection fraction
IL1RL1	interleukin-1 receptor-like 1
IMAC-2	Intervention in Myocarditis and Acute Cardiomyopathy-2

LVEF	left ventricular ejection fraction
MKI67	marker of proliferation Ki-67
MMP2	matrix metalloproteinase 2
PDGF	platelet-derived growth factor
PDGF-BB	PDGF subunit B homodimer
PDGFR	PDGF receptor
RNA-seq	RNA sequencing
SNP	single-nucleotide polymorphism
ST2	suppression of tumorigenicity-2
sST2	soluble ST2
TGF-β	transforming growth factor beta
VIM	vimentin

dilated cardiomyopathy (DCM) is the most common cause of heart transplantation, accounting for 30% to 40% of all cases of HFrEF. Treatment response is highly variable among individuals with DCM, with some patients having little or no clinical response to standard drug therapy.⁴ Change in left ventricular ejection fraction (LVEF) that

occurs during drug therapy correlates significantly with mortality, and, therefore, it serves as a reliable surrogate measurement for mortality in DCM and for assessing myocardial recovery in response to pharmacotherapy.⁵

Genome-wide association studies (GWAS), by adopting an agnostic approach, could provide insight into novel biological pathways that, in turn, could affect drug utilization and the development of novel drug therapy. An analysis of GWAS-identified genes for drug repositioning demonstrated that a large number of these genes are targeted by drugs that have indications closely related to the GWAS trait or have indications different from the GWAS trait and, thus, can be repositioned as immediate translational opportunities.⁶ The genomic revolution, however, has had limited therapeutic success in HFrEF. Although case-control GWAS studies have identified DCM susceptibility genes,⁷ there have been no genomic studies assessing treatment response in DCM, which, if performed, could potentially have direct therapeutic implications.

In the present study, we first performed a discovery GWAS for change in LVEF in 686 White subjects with recent-onset DCM who received standard pharmacotherapy. The GWAS identified a single-nucleotide polymorphism (SNP) signal mapping to the 5'-flanking region of *CDCP1* (CUB [complement C1r/C1s, Uegf, and Bmp1] domain containing protein 1), a gene that had previously been reported to play a role in pulmonary fibrosis and bone marrow fibroblasts,^{8,9} but its possible function in cardiac fibrosis is unknown. Cardiac fibrosis is a histological hallmark of DCM and surpasses LVEF as a prognostic marker in heart failure.¹⁰ Therefore, in follow-up of the GWAS, we performed extensive functional genomic studies that demonstrated that *CDCP1* plays a role in regulating human cardiac fibroblast (HCF) proliferation through PDGF (platelet-derived growth factor) signaling and mitosis. Finally, RNA sequencing (RNA-seq) analysis after *CDCP1* knockdown in HCFs made it possible to identify transcriptome-wide differentially expressed genes (DEGs), including significant downregulation of the *IL1RL1* (interleukin-1 receptor-like 1) gene, which encodes soluble ST2 (suppression of tumorigenicity-2; sST2), an inductor of heart failure and cardiac fibrosis.^{11,12} In summary, the application of a discovery GWAS followed by in-depth functional genomic studies—a strategy that we have applied previously with repeated success^{13–16}—identified *CDCP1* as a novel target that is associated with myocardial recovery in DCM and which may modulate cardiac fibrosis.

METHODS

Data Availability

The RNA-seq data generated in this study have been deposited in National Center for Biotechnology Information's (NCBI) Gene Expression Omnibus and are accessible through Gene Expression Omnibus Series accession number GSE222695.

DCM Population

Patients were recruited in multiple medical institutions including participant institutions of the IMAC-2 study (Intervention in Myocarditis and Acute Cardiomyopathy-2),⁴ the Mayo Clinic, University of Colorado School of Medicine, University of Trieste (Italy), Mario Negri Institute for Pharmacological Research (Italy), CHU de Lille (France),^{17,18} and St. Anne's University Hospital (Czech Republic). All subjects had DCM with LVEF $\leq 50\%$ in whom coronary artery disease or other secondary causes of HFrEF were excluded and who were diagnosed within 6 months of developing symptoms. The detailed inclusion and exclusion criteria are outlined in [Figure S1](#). Patients had echocardiograms performed within 30 days of their diagnosis at baseline, and follow-up echocardiograms were performed after a median of 6 months of treatment with ACE (angiotensin-converting enzyme) inhibitors or angiotensin 2 receptor blocker and β -blockers. All patients provided written informed consent to have blood samples drawn for DNA extraction and analyses. The study was reviewed and approved by the Mayo Clinic Institutional Review Board and the institutional review boards of the respective participating institutions.

GWAS Analysis

Patient DNA samples were genotyped using Illumina Human 610-Quad BeadChips, as described previously.^{13–15} Change in LVEF after drug treatment was used as a phenotype. Approximately 7.87 million observed and imputed SNPs were analyzed using PLINK linear regression, with adjustment of covariates (baseline LVEF, sex, age, time to follow-up echocardiogram, and recruiting site). See the [Supplemental Methods](#) for details.

Fine-Mapping of the Chromosome 3 SNP Signal

SNP function was annotated using public multiomics data sets. The expression quantitative trait locus information was obtained from the Gene-Tissue Expression Project.¹⁹ The data sets for annotation of regulatory DNA elements were obtained from the Encyclopedia of DNA Elements Project.²⁰ Those sequence-based data were visualized using the interactive genome viewer.²¹ The sources of these sequencing data sets and other resources used in this study are listed in the [Major Resources Table](#).

SNP/Gene Functional Studies in HCFs

See the [Supplemental Methods](#) for detailed methods. Briefly, the effect of the GWAS-identified SNP locus on gene transcriptional activity was tested by reporter gene assay. Genes of interest were knocked down in HCFs by siRNA and were overexpressed by cDNA construct transfection. HCF cell proliferation was measured by MTS (3-(4,5-dimethylthiazol-2-yl)-5-(3-carboxymethoxyphenyl)-2-(4-sulfophenyl)-2H-tetrazolium) assays after knockdown or growth factor treatment. Reverse transcription-quantitative PCR (RT-qPCR) was used for quantification of mRNA levels and Western blots for proteins. Immunofluorescence staining was performed to visualize protein targets in HCFs. RNA-seq was performed for quantification of transcriptome-wide gene expression level in HCFs. *CDCP1*-related DEGs were identified by comparing RNA-seq results of control to that of the *CDCP1* knockdown group. Those DEGs were then subjected to pathway analysis for annotation of *CDCP1* function.

RESULTS

DCM Patient Characteristics

A total of 686 patients with recent-onset DCM were enrolled in the final GWAS analysis. Their clinical characteristics are outlined in Table S1. After a period of pharmacotherapy, follow-up LVEF measurements were obtained at a median time of 6 months, demonstrating an average improvement in LVEF of 43%. LVEF measured at baseline (V_1) and after pharmacotherapy (V_2) is plotted in Figure 1A, demonstrating a variable myocardial recovery in response to pharmacotherapy. Change in LVEF ($V_2 - V_1$) in these 686 patients showed a gaussian distribution (Figure 1B) and was used as the phenotype for the GWAS analysis after adjustment for covariates.

GWAS for Changes in LVEF in DCM Patients

The Manhattan plot showing SNP associations with changes in LVEF after drug treatment is presented in Figure 2A. The Q-Q plot for the GWAS analysis did not show evidence of genomic inflation ($\lambda=0.991$) and is shown in Figure S2A. SNPs with suggestive significant associations ($P < 10^{-5}$) are listed in Table S2. Although none of the SNPs reached genome-wide significant associations ($P < 5.0 \times 10^{-8}$), there were 2 SNPs with the lowest P values, which were highly suggestive ($P < 10^{-6}$; Figure 2A). A locus zoom plot for the chromosome 3 SNPs showed that the top SNP, rs6773435 (G>T), mapped 5'-upstream of *TMEM158* (transmembrane protein 158) and linked SNPs covered a DNA region that included the

TMEM158 gene and the 5'-flanking region of a nearby gene *CDCP1* (Figure 2B). The other highly suggestive SNP (rs11105445) on chromosome 12 mapped to an intergenic region (Figure S2B). The GWAS analysis also showed that the minor alleles for both the chromosome 3 and chromosome 12 SNPs were associated with positive β values (Table S2), indicating that the variant alleles for both SNPs were associated with increased LVEF or myocardial recovery after drug treatment. More significant genotype-dependent changes in LVEF were observed when both SNP genotypes were combined, that is, compared with patients who had wild-type genotypes for both SNPs ($n=206$), patients who had heterozygous genotypes for both SNPs ($n=82$) were estimated to have 6.07 (95% CI, 3.81–8.34) units improvement in LVEF (Table S3).

Although the SNP signals identified in the GWAS are highly suggestive while not genome-wide significant, it is well known that the value of biological insight gained from GWAS is not necessarily proportional to the strength of statistical association. This concept has been proven by prior GWAS reported by us^{13–16} and other groups,^{22,23} in which SNP loci with highly suggestive associations have revealed important biological mechanisms related to the GWAS phenotype with the pursuit of functional genomic studies. To further validate our GWAS findings, we performed functional genomic studies starting with the chromosome 3 SNP signal since it mapped close to a gene-coding region (Figure 2B). As described subsequently, we found that *TMEM158* is a pseudogene and that its DNA sequence includes an enhancer that influences *CDCP1* transcription.

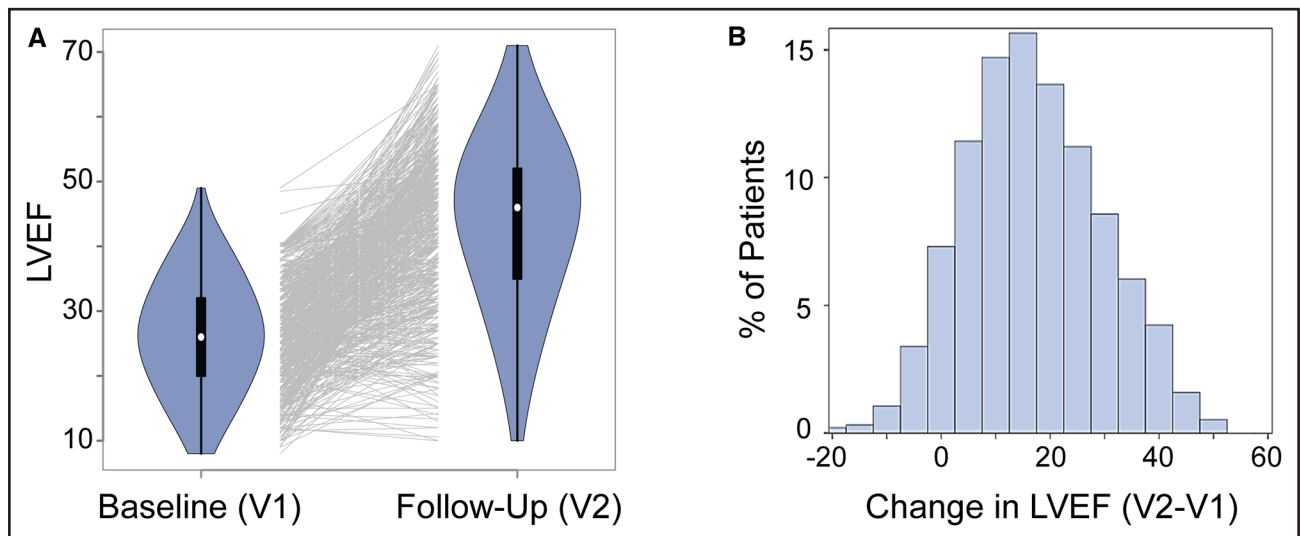


Figure 1. Myocardial recovery in recent-onset dilated cardiomyopathy (DCM) measured by left ventricular ejection fraction (LVEF).

A, Violin plots that show LVEF data for 686 patients with DCM at baseline (V_1) and at follow-up after pharmacotherapy (V_2). Each line in the middle of the plot links LVEF data for an individual patient at V_1 and V_2 . Many of the patients had their LVEFs increase, but for some patients, LVEF values did not change or decrease after pharmacotherapy. **B**, Distribution of changes in LVEFs in these 686 patients after pharmacotherapy.

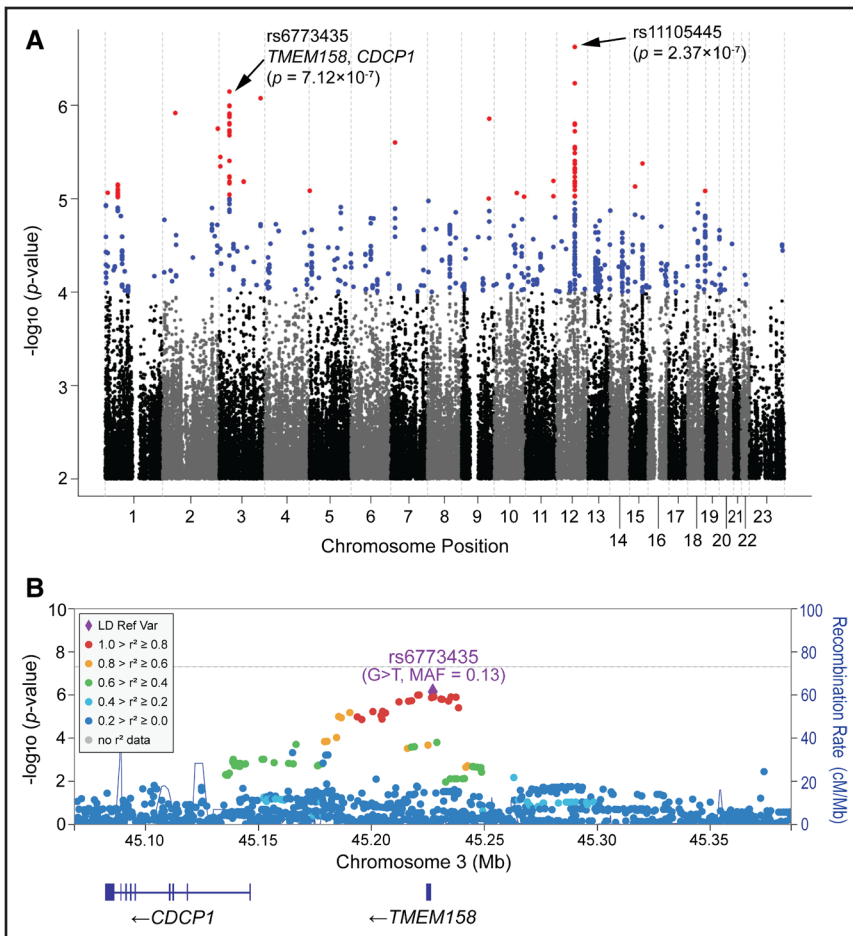


Figure 2. Genome-wide association study (GWAS) for changes in left ventricular ejection fraction (LVEF) in dilated cardiomyopathy (DCM).

A, Manhattan plots for the GWAS of changes in LVEFs in 686 patients with DCM who received pharmacotherapy. Two top single-nucleotide polymorphisms (SNPs) on chromosomes 12 and 3 have been highlighted. **B**, Regional association (locus zoom) plot for the chromosome 3 SNP signal. The color of each SNP represents its linkage disequilibrium (LD) in a European population (the 1000 Genomics Project) with the reference SNP rs6773435, which is colored purple. MAF indicates minor allele frequency.

Fine-Mapping of the Chromosome 3 SNP Signal Revealed a Potential Role for *CDCP1* in Cardiac Fibrosis

The chromosome 3 SNP locus, which covers the entire *TMEM158* gene (Figure 2B), has been annotated as a candidate *cis*-regulatory DNA element in heart left ventricular tissue and HCFs by the Encyclopedia of DNA Elements²⁰ (Figure 3A). Specifically, the SNP locus has been annotated as an accessible chromatin site (by the assay for transposase-accessible chromatin with sequencing [ATAC-seq] or DNase-seq data), promoter (by H3K4me3 [Trimethylation of Histone H3 at Lysine 4] chromatin immunoprecipitation sequence [ChIP-seq]), enhancer (by H3K27ac [Histone 3 lysine 27 acetylation] ChIP-seq), and chromatin looping site (by CTCF [CCCTC-Binding Factor] ChIP-seq; Figure 3A), indicating that this locus might modulate gene transcriptional regulation. The top SNP, rs6773435, is an expression quantitative trait locus for both *TMEM158* and *CDCP1* in several tissues and cell lines¹⁹ (Figure S3), but whether it might affect gene transcription in human heart cells requires further functional studies.

We first excluded the *TMEM158* gene from our functional studies since we found that *TMEM158* is a pseudogene that does not encode protein.

Specifically, RNA-seq data generated by the Gene-Tissue Expression Project¹⁹ demonstrated that, even though *TMEM158* RNA is expressed in multiple human tissues and cell lines, intact *TMEM158* mRNA is not found in any human tissue or cell line. More specifically, a region of the *TMEM158* open reading frame has no RNA-seq reads that have been observed in heart left ventricular tissue, in HCFs (Figure 3B, red arrows) or in tissues/cells in which *TMEM158* RNA is most highly expressed (Figure S4, red arrows). These RNA-seq read mapping results suggest that an intact *TMEM158* mRNA does not exist; thus it cannot be translated to protein. We also attempted to detect the putative *TMEM158* protein by Western blot. To generate a positive control for the Western blot assay, a FLAG-tagged *TMEM158* fusion protein was overexpressed and confirmed by anti-FLAG antibody (Figure 3C). Control samples were then loaded with protein lysates from HCFs and blotted with the anti-*TMEM158* antibody (Figure 3D). As expected, no *TMEM158* protein was detectable in HCFs (Figure 3D). It is possible that the *TMEM158* RNA is an enhancer RNA that is transcribed at active enhancers²⁴ since the entire *TMEM158* locus has been annotated as enhancers (Figure 3A). As a result of these observations, we focused our attention on the *CDCP1* gene and tested the hypothesis that its

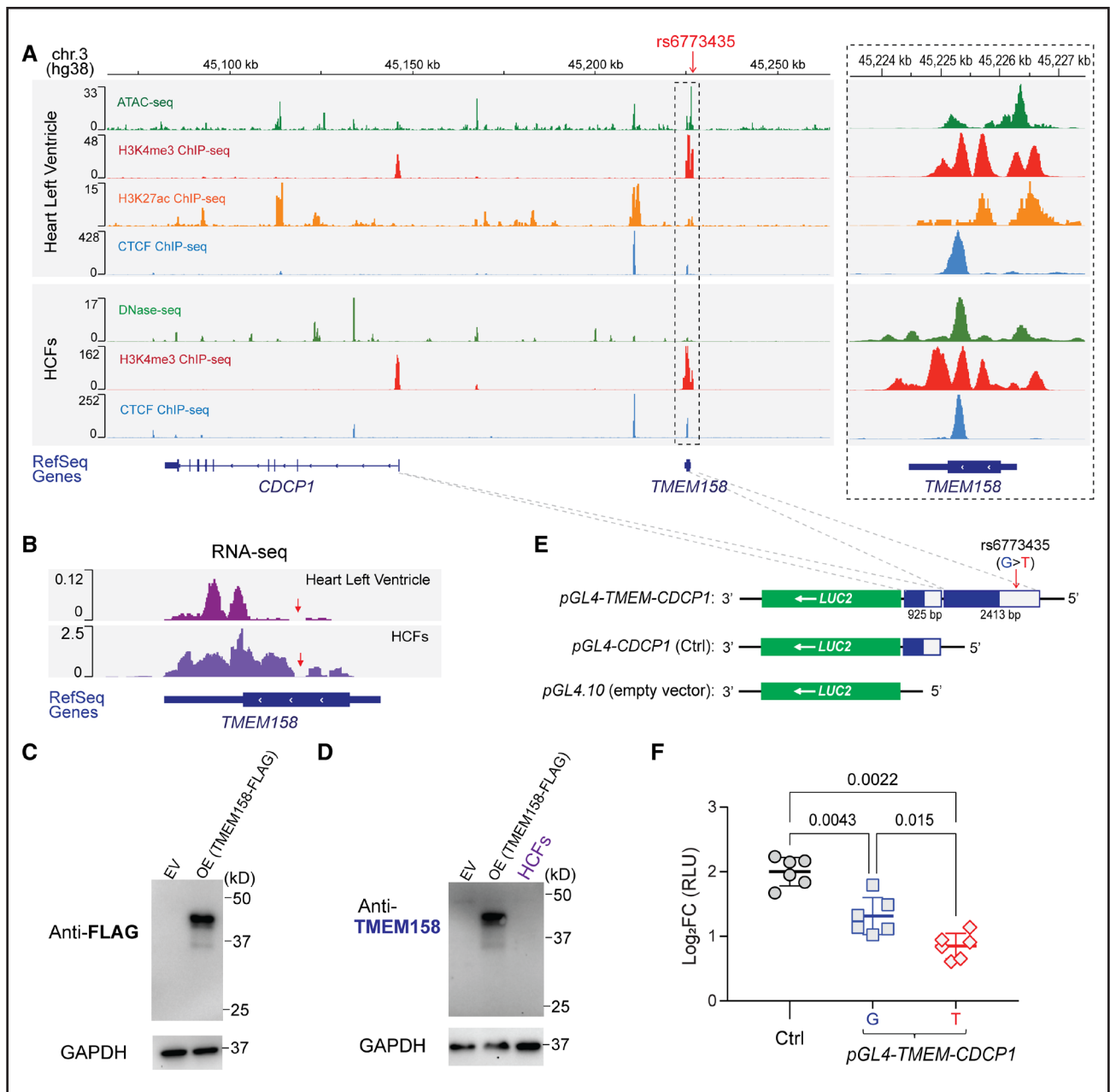


Figure 3. Functional annotation of the chromosome 3 single-nucleotide polymorphism (SNP) locus.

A, Visualization of the ENCODE epigenomic data set in the interactive genome viewer (IGV). From **top to bottom** shows the physical position of the rs6773435 SNP locus on chromosome 3 based on human genome assembly (hg38); assay for transposase-accessible chromatin with sequencing [ATAC-seq] to assess genome-wide chromatin accessibility, chromatin immunoprecipitation sequence (ChIP-seq) for H3K4me3 (Trimethylation of Histone H3 at Lysine 4; promoter marker), for H3K27ac (Histone 3 lysine 27 acetylation; enhancer and promoter marker), and for CTCF (CCCTC-Binding Factor; chromatin looping marker) that were generated using human left ventricular tissues; DNase-seq to assess genome-wide chromatin accessibility, ChIP-seq for H3K4me3, and for CTCF that were generated using human cardiac fibroblasts (HCFs; ATAC-seq and H3K27ac ChIP-seq data are not available for the HCFs). Genes were annotated by the National Center for Biotechnology Information (NCBI) human genome RefSeq. Both the *TMEM158* and *CDSCP1* genes are transcribed from the negative DNA strand. The dashed box on the **right** is a zoom-in of the SNP locus. Sequencing peaks are mapped to the SNP locus, which indicates that the locus is likely a transcriptional activating site. **B**, RNA sequencing (RNA-seq) reads generated from human heart left ventricular tissue and HCFs, which map to the *TMEM158* gene annotated by RefSeq. The *TMEM158* open reading frame (ORF) and untranslated region (UTR) were depicted by thick and thin lines, respectively. Red arrows indicate a region of the *TMEM158* ORF where no RNA-seq reads were mapped. **C**, Western blots using an anti-FLAG antibody for the putative *TMEM158*-FLAG fusion protein after overexpression (OE) in HEK-293T cells. Empty vector (EV) control sample was obtained from cells transfected with pCMV-entry plasmid. **D**, Western blot using anti-*TMEM158* antibody for endogenous *TMEM158* protein in HCFs. Overexpressed *TMEM158*-FLAG fusion protein sample, as same as which is blotted in **C** with anti-FLAG antibody, was blotted with the anti-*TMEM158* antibody, which successfully detects overexpressed *TMEM158*-FLAG fusion protein. However, no endogenous *TMEM158* protein was detected in protein lysates from HCFs. **E**, Construction of reporter gene plasmids. The *pGL4.10* plasmid, which includes an *LUC2* reporter gene, was used as the backbone construct and served as an empty vector control. The *CDSCP1* promoter region (925 bp) was (Continued)

expression might be regulated by the *TMEM158* and rs6773435 SNP locus.

To determine whether the rs6773435 SNP (G>T) might affect *CDCP1* transcription in HCFs, DNA fragments containing that SNP locus and the *CDCP1* promoter were cloned into the *pGL4.10* luciferase reporter gene plasmid (Figure 3E). A construct with the *CDCP1* promoter was cloned and served as control. Those plasmids were then transfected into HCFs, and luciferase activity was quantified and normalized to that of the *pGL4.10* plasmid (empty vector). Increased luciferase activity was observed in HCFs transfected with those plasmids when compared with empty vector (Figure 3F; log₂ fold change, >0). The control plasmid that contained only the *CDCP1* promoter displayed the greatest increase in luciferase activity compared with plasmids containing the rs6773435 SNP locus, suggesting that the SNP locus negatively regulates *CDCP1* transcription. Importantly, we also observed that plasmids containing the rs6773435 SNP T allele resulted in smaller increases in luciferase activity (Figure 3F), indicating that the variant T allele may result in less *CDCP1* transcription as compared with the common G allele.

CDCP1 encodes a single-pass transmembrane glycoprotein, CDCP1, which has been studied extensively in cancer^{25–30} and immune-related diseases.^{31–33} We reviewed the expression of *CDCP1* in various tissues included in the Gene-Tissue Expression portal.¹⁹ The results indicated that *CDCP1* had minimal expression in myocardial tissue but is expressed in cultured fibroblasts (Figure S5). CDCP1 has also been reported to modulate pulmonary fibrosis,⁸ but its role in cardiac fibrosis is unknown. We also consulted the phenotype-wide association study based on the UK Biobank data sets (<https://pheweb.org/UKB-Neale/>), which showed that genetic variants in/near the *CDCP1* gene have been significantly associated with heart failure mortality (Figure S6) and with death due to thoracic aneurysm rupture (Figure S7). In summary, this series of studies of the chromosome 3 SNP signal formed the basis for our investigation of the role of *CDCP1* in myocardial fibrosis and recovery.

CDCP1 Is Required for HCF Proliferation

CDCP1 expression is known to be significantly upregulated in a variety of cancers and appears to drive cancer cell growth and metastasis.^{25–30} Inspired by the molecular function of CDCP1 in cancer, we set out to determine

whether CDCP1 might affect HCF cell growth. *CDCP1* knockdown in primary HCFs (Figure 4A, left; Figure 4B) can significantly suppress cell proliferation (Figure 4C). We also demonstrated that *TMEM158* knockdown (Figure 4A, right) had no effect on HCF proliferation (Figure 4C), likely because the *TMEM158* protein is not translated from its RNA (Figure 3B and 3D). To further validate this observation, we performed *CDCP1* overexpression experiments in HCFs and found that it promotes HCF proliferation (Figure S8), an expected opposite direction observed in the *CDCP1* knockdown experiments, confirming the role of CDCP1 in HCF proliferation.

We also noted that baseline CDCP1 expression is low in primary HCFs, for example, based on the RT-qPCR assay, *CDCP1* mRNA level is about 0.2% to 2% of GAPDH, and it required a significantly longer exposure time to see CDCP1 than GAPDH bands in Western blots of HCFs (Figure 4B). However, CDCP1 is known to be induced by activation of PDGF signaling in cancer cells,²⁷ and PDGF signaling is also known to induce cardiac fibrosis.^{34–37} To determine whether CDCP1 might also be induced in HCFs, those cells were starved in serum-deprived media and were then treated with PDGF-BB (PDGF subunit B homodimer), which activates both PDGFRs (PDGF receptors) α and β . We found that the mRNA levels of CDCP1, as well as the MKI67 (marker of proliferation Ki-67), were significantly induced in HCFs after PDGF-BB treatment in a dose-dependent manner (Figure 4D). The CDCP1 protein was also increased after PDGF-BB treatment (20 ng/mL) in a time-dependent manner, with a significantly higher CDCP1 protein level observed after 48 hours of treatment (Figure 4E and 4F). As expected, phosphorylated PDGFR α , a marker of PDGF signaling activation, as well as downstream PDGF signaling proteins, phosphorylated AKT (protein kinase B) and phosphorylated ERK1/2 (extracellular signal-regulated kinase 1/2), were significantly upregulated after PDGF-BB treatment (Figure 4E). CDCP1 induction by PDGF-BB was also visualized in HCFs by coimmunostaining with the fibroblast marker VIM (vimentin), which showed that longer fibers were stretched out from HCFs after PDGF-BB treatment (Figure 4G). Meanwhile, proliferation of HCFs cultured in serum-deprived media was significantly promoted by PDGF-BB treatment, compared with vehicle treatment, which, as expected, did not proliferate due to lack of growth factors in serum-deprived media (Figure 4H). Of

Figure 3 Continued. cloned into the 5'-end of the *LUC2* reporter gene and was used as a positive control plasmid (*pGL4-CDCP1*) for *CDCP1* transcriptional activity. To test the effect of the rs6773435 SNP locus on *CDCP1* transcription, DNA fragments that included the rs6773435 SNP/*TMEM158* locus (2413 bp) were cloned into the 5'-end of *pGL4-CDCP1* (*pGL4-TMEM-CDCP1*). The *pGL4-TMEM-CDCP1* plasmid containing the rs6773435 SNP G allele was compared with that containing the T allele. **F**, Comparison of luciferase activities in HCFs transfected with *pGL4.10* (empty vector), *pGL4-CDCP1* (Ctrl), *pGL4-TMEM-CDCP1* G, and *pGL4-TMEM-CDCP1* T. Data are log₂ fold change (FC) in relative light units (RLUs) when compared with *pGL4.10* alone (empty vector) from biological replicates (n=6) showing as mean values \pm SD. The Mann-Whitney *U* test was used to calculate the presented *P* values.

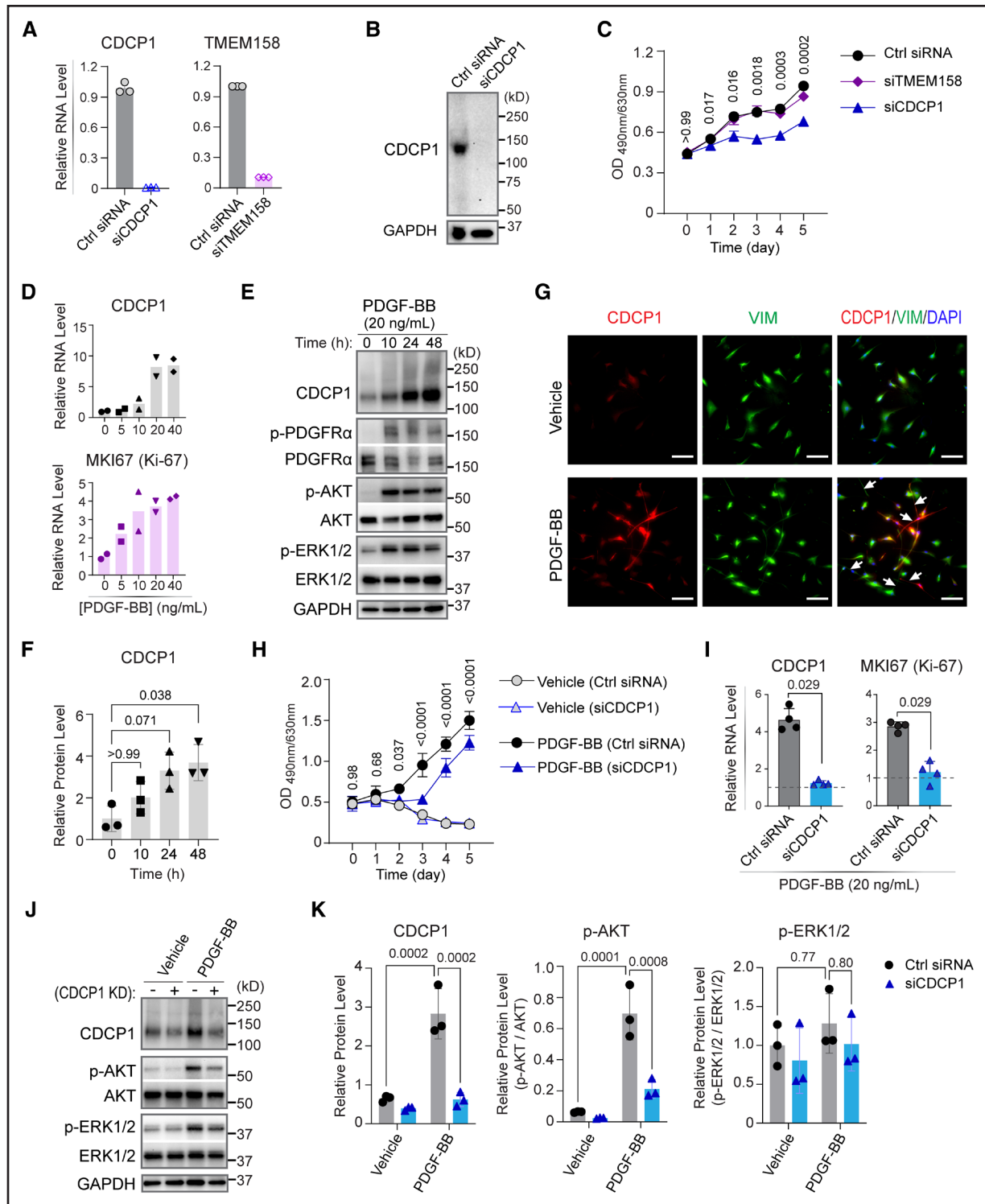


Figure 4. CDCP1 (CUB domain containing protein 1) is required for human cardiac fibroblast (HCF) proliferation.

A, Reverse transcription-quantitative PCR (RT-qPCR) quantification of CDCP1 and TMEM158 mRNA levels in HCFs 48 hours after knockdown by specific siRNAs. GAPDH mRNA levels were quantified as internal control. Data shown are triplicate quantification of same samples. **B**, Western blot assay for CDCP1 in HCFs transfected with CDCP1 siRNA (siCDCP1). GAPDH was blotted as an internal control. **C**, HCF cell proliferation assays. Cells were transfected with siRNAs at day 0, and cell viability was measured by an MTS (3-(4,5-dimethylthiazol-2-yl)-5-(3-carboxymethoxyphenyl)-2-(4-sulfophenyl)-2H-tetrazolium) assay every 24 hours until day 5. Each dot is a mean value for 3 independent experiments ($n=3$). Error bars represent SDs. Statistical analysis by 2-way ANOVA with Tukey multiple comparisons test. P values are shown for comparisons of Ctrl siRNA to siCDCP1 groups. **D**, CDCP1 and MKI67 (marker of proliferation Ki-67) mRNA levels were quantified by RT-qPCR in HCFs after 24-hour treatments with PDGF-BB (platelet-derived growth factor subunit B homodimer) at different concentrations. Plots are showing duplicate RT-qPCR assays using GAPDH as an internal control. **E**, Western blot assay for CDCP1 in HCFs incubated with 20 ng/mL of PDGF-BB at different time points. Phosphorylated PDGFR α (platelet-derived growth factor receptor α ; p-PDGFR α) (Continued)

importance, knockdown of *CDCP1* repressed PDGF-BB-stimulated HCF proliferation (Figure 4H), as well as the transcription of *MKI67* (Figure 4I), supporting the hypothesis that *CDCP1* induction is required for HCF proliferation stimulated by PDGF-BB. We also found that *CDCP1* knockdown significantly decreases phosphorylated AKT, which promotes cell proliferation and cell cycle³⁸ in HCFs with or without PDGF-BB treatment (Figure 4J and 4K), suggesting that the decreased HCF proliferation after *CDCP1* knockdown could be linked to attenuated AKT phosphorylation.

In addition to proliferation, cardiac fibroblast-to-myofibroblast transdifferentiation is an important step in the development of cardiac fibrosis.^{34–36} After HCFs were treated with PDGF-BB, there was no change in expression of *ACTA2*, which encodes α -SMA (alpha-smooth muscle actin; a marker of myofibroblasts; Figure S9A), indicating that PDGF-BB treatment has little or no effect on myofibroblast transdifferentiation. Consistent with this finding, *CDCP1* knockdown had no effect on α -SMA expression after PDGF-BB treatment (Figure S9B through S9D), despite significant repression of *MKI67* (Figure 4I), indicating that *CDCP1* plays an important role in HCF proliferation, but it may not influence cardiac myofibroblast transdifferentiation.

CDCP1 Has a Limited Role in TGF- β 1-Induced Cardiac Fibroblast-to-Myofibroblast Transdifferentiation

Fibroblast-to-myofibroblast transdifferentiation is well known to be stimulated by TGF- β (transforming growth factor beta) signaling.^{34,35} To further investigate whether *CDCP1* plays a role in TGF- β 1-induced cardiac fibroblast-to-myofibroblast transdifferentiation, HCFs were stimulated by TGF- β 1 in serial concentrations (Figure 5A) or time courses (Figure 5B). *ACTA2* expression, as expected, increased after TGF- β 1 treatment while *CDCP1* expression, as well as that of *MKI67*, was decreased (Figure 5A and 5B). The decrease in *CDCP1* expression after TGF- β 1 treatment has also

been observed in human lung fibroblasts.⁸ This decrease in *CDCP1* expression is most likely a result of repressed cell proliferation, as indicated by decreased *MKI67* expression, which would be expected when transdifferentiation occurs after TGF- β 1 treatment. It is known that myofibroblast transdifferentiation stops fibroblast proliferation, for example, the marker of myofibroblast, α -SMA, is also named cell growth-inhibiting gene 46 protein. Finally, *CDCP1* knockdown had no effect on the protein expression of phosphorylated SMAD2 (Suppressor Mothers Against Decapentaplegic 2), α -SMA, COL1A1 (collagen type I alpha 1 chain), FN-1 (fibronectin-1), COL5A1 (collagen type 5 alpha 1 chain), and MMP2 (matrix metalloproteinase 2), or the percentage of α -SMA+ cells, which were significantly upregulated by 48 hours of TGF- β 1 treatment (Figure S10), indicating that *CDCP1* has no effect on TGF- β 1-mediated myofibroblast transdifferentiation.

Because *CDCP1* baseline expression in HCFs is relatively low and is decreased after TGF- β 1 treatment, we performed *CDCP1* overexpression experiments in HCFs to validate observations made with *CDCP1* knockdown and TGF- β 1 treatment (Figure S10). To capture a dynamic change in fibroblast-to-myofibroblast transdifferentiation, protein samples were collected from HCFs with *CDCP1* overexpression at both 24 and 72 hours of TGF- β 1 treatment. As expected, protein levels of phosphorylated SMAD2, α -SMA, COL1A1, and FN-1 were significantly upregulated in those cells with 24 hours of TGF- β 1 treatment (Figure 5C). When comparing the *CDCP1* overexpression to empty vector control groups, a small decrease in α -SMA and FN-1 protein levels was observed in *CDCP1* overexpression cells at 24 hours but not after 72 hours of TGF- β 1 treatment (Figure 5C and 5D). However, the phosphorylated SMAD2 level, a marker of TGF- β signaling activation, did not differ from *CDCP1* overexpression to empty vector control groups at both 24 and 72 hours of TGF- β 1 treatment, suggesting that *CDCP1* has no effect on TGF- β signaling activation.

Phosphorylation of SMAD2/3 often responds immediately to TGF- β stimulation. To further investigate

Figure 4 Continued. was blotted as control of PDGF-BB treatment. Two known PDGFR downstream signaling proteins, phosphorylated AKT (protein kinase B; p-AKT) and phosphorylated ERK1/2 (extracellular signal-regulated kinase 1/2; p-ERK1/2), were also blotted. GAPDH was blotted as internal control. **F**, *CDCP1* protein level quantified from independent Western blot experiments (n=3) as represented in **E**. *CDCP1* bands were normalized to that of GAPDH and then control treatment (0 h). *P* values were calculated by Kruskal-Wallis test with Dunn multiple comparisons to 0 hours of PDGF-BB treatment. **G**, Immunofluorescence staining of *CDCP1* and HCF marker, VIM (vimentin), in HCFs after 24-hour treatments with vehicle or PDGF-BB. HCF morphology was changed with long fibers (arrow heads) and can be seen after PDGF-BB treatment. Scale bars represent 200 μ m. **H**, HCF cell proliferation in starving (serum deprived) media supplied without (vehicle) or with 20 ng/mL of PDGF-BB. Cells were transfected with siRNAs at day 0, and cell viability was measured by an MTS assay every 24 hours until day 5. Each dot is a mean value for 3 independent assays. Error bars represent SD. Statistical analysis by 2-way ANOVA with Tukey multiple comparisons test. *P* values are shown for comparisons of Ctrl siRNA to si*CDCP1* in the PDGF-BB treatment groups. **I**, *CDCP1* and *MKI67* mRNA levels were quantified by RT-qPCR in HCFs 48 hours after *CDCP1* knockdown and PDGF-BB treatment, with GAPDH mRNA level as internal control. RNA levels were normalized to vehicle treatment (dashed line). Data are mean values \pm SD for independent experiments (n=4). The Mann-Whitney *U* test was used to calculate the presented *P* values. **J**, Western blot assay for *CDCP1* and PDGFR downstream signaling proteins (p-AKT and p-ERK1/2) in HCFs with *CDCP1* knockdown (KD) and 20 ng/mL of PDGF-BB treatment. GAPDH was blotted as internal control. **K**, Protein levels quantified from 3 independent samples by Western blot assays as represented in **J**. Protein bands were normalized to that of GAPDH. Levels of p-AKT and p-ERK1/2 were showed as ratios to their total protein level. *P* values were calculated by ordinary 1-way ANOVA with Tukey multiple comparisons test.

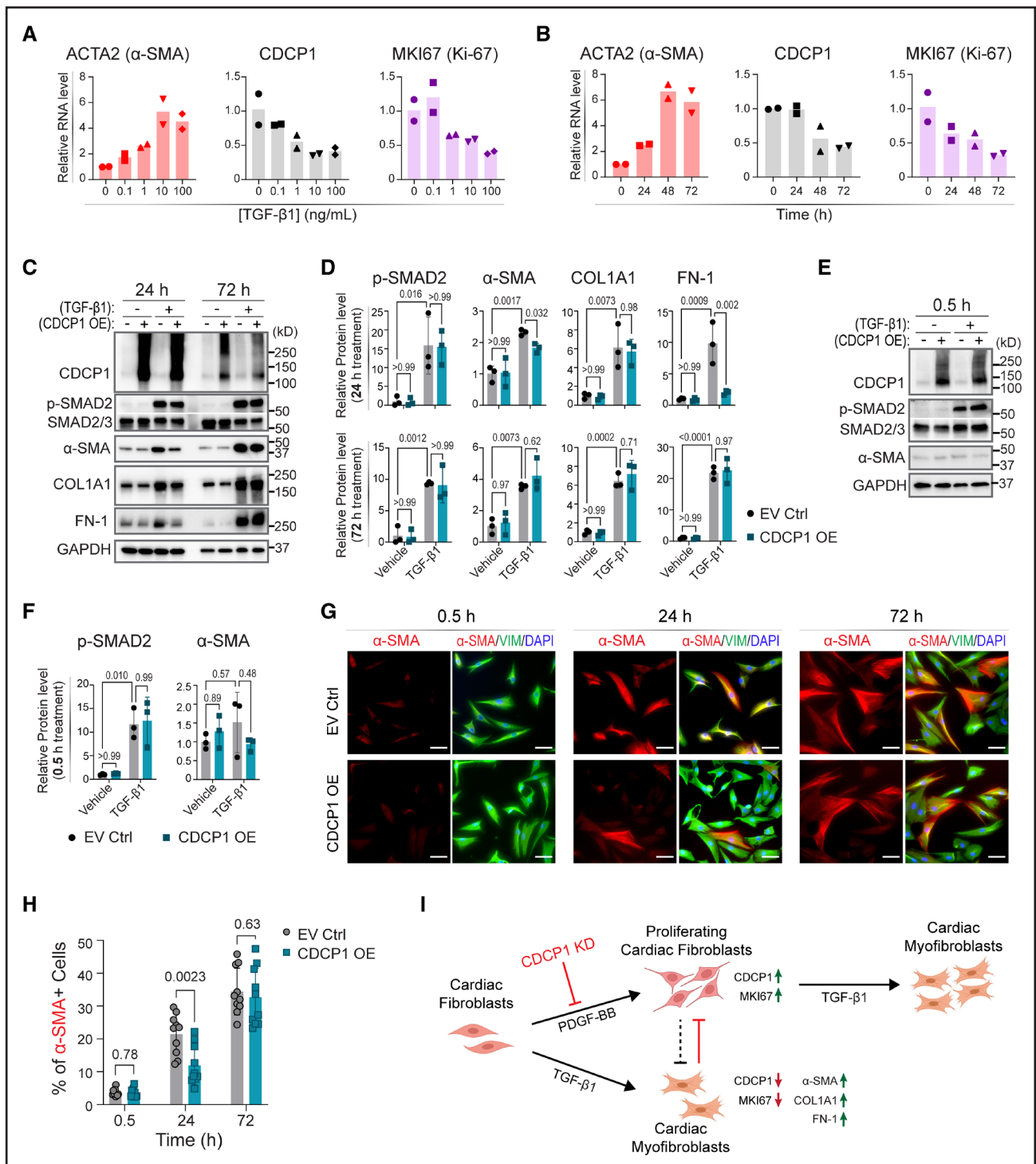


Figure 5. CDCP1 (CUB domain containing protein 1)-induced and TGF- β 1 (transforming growth factor beta-1)-induced cardiac fibroblast-to-myofibroblast transdifferentiation.

A, Relative mRNA levels of ACTA2 (Actin Alpha 2), CDCP1, and MKI67 (marker of proliferation Ki-67) in human cardiac fibroblasts (HCFs) after 48-hour treatment of TGF- β 1 at different concentrations and **(B)** after 10 ng/mL of TGF- β 1 treatment at different time (h). RNA levels were quantified by reverse transcription-quantitative PCR (RT-qPCR) with GAPDH level as internal control from duplicate assays. **C**, Western blot for CDCP1 and other protein markers in HCFs with or without CDCP1 overexpression (OE) and with or without TGF- β 1 treatment (10 ng/mL) at 2 time points (24 and 72 h of treatment). Phosphorylated SMAD2 (Suppressor Mothers Against Decapentaplegic 2; p-SMAD2) and α -SMA (alpha-smooth muscle actin) were blotted for control of TGF- β 1 treatment and myofibroblast transdifferentiation, respectively. ECM (extracellular matrix) proteins including COL1A1 (collagen type I alpha 1 chain) and FN-1 (fibronectin-1) were also blotted. GAPDH was blotted as internal control. **D**, Relative protein level quantified from 3 independent samples by Western blot assays as represented in **C**. Protein levels were normalized to GAPDH level and then to vehicle and empty vector control (EV Ctrl) sample. Error bars represent SDs of triplicate assays. *P* values were calculated by ordinary 1-way ANOVA with Tukey multiple comparisons test. **E**, Western blot for CDCP1, p-SMAD2, and α -SMA in HCFs (*Continued*)

whether CDCP1 affects TGF- β 1 signaling in HCFs, cells with *CDCP1* overexpression were treated with TGF- β 1 for only 0.5 hours, which is sufficient to induce SMAD2 phosphorylation (Figure 5E). However, CDCP1 overexpression had no effect on phosphorylated SMAD2 levels induced at 0.5 hours by TGF- β 1 treatment (Figure 5E and 5F), a result that once again supports the observation that CDCP1 has no effect on TGF- β 1 signaling. No induction of α -SMA was observed within this time period (0.5 hours) of TGF- β 1 treatment (Figure 5E and 5F).

Finally, cells with *CDCP1* overexpression were coimmunostained with α -SMA and VIM, and the number of α -SMA+ cells was counted. Consistent with the Western blot result, the percentage of α -SMA+ cells in the *CDCP1* overexpression group was less at 24 hours but did not differ after 72 hours of TGF- β 1 treatment (Figure 5G and 5H). These observed decreases in the α -SMA level and in percentage of α -SMA+ cells at 24 hours of TGF- β 1 treatment in the *CDCP1* overexpression group are likely a result of *CDCP1* overexpression-induced HCF proliferation (Figure S8) that precedes and hence delays myofibroblast transdifferentiation.

In summary, we demonstrated that CDCP1 is significantly induced in HCFs after PDGF-BB treatment and is required for HCF proliferation (Figures 4 and 5I), but that it might have little or no effect on cardiac fibroblast-to-myofibroblast transdifferentiation stimulated by TGF- β 1 (Figure 5).

Transcriptomic Profiling of *CDCP1* Knockdown in HCFs Revealed Its Role in Regulation of *SST2* Expression

To further investigate CDCP1 molecular mechanisms, we performed RNA-seq assays after the knockdown of CDCP1 in HCFs. Transcriptome-wide DEGs were identified (Figure 6A), followed by pathway enrichment analyses using those DEGs (Figure 6B). A total of 1061 DEGs with fold changes of >2 ($|\log_2$ fold change >1.0 ; false discovery rate, <0.05) after CDCP1 knockdown were identified (Table S4). When those DEGs were subjected to gene ontology pathway enrichment analysis, as expected, regulation of cell population proliferation was identified as

one of the top biological process pathways (Figure 6B), a pathway that helps explain our observation that CDCP1 is required for HCF proliferation (Figure 4). Consistently, pathways related to cell cycle and mitosis, which play important roles during cell proliferation, were also enriched by CDCP1-mediated DEGs (Figure 6B). The gene ontology enrichments for molecular function and cellular component pathways support a role for CDCP1 in the regulation of mitosis, for example, the top enriched molecular function is microtubule binding and the top enriched cellular component is spindle (Figure S11).

In addition to pathway enrichment analysis, our RNA-seq data made it possible to identify specific genes for which expression was affected by CDCP1 knockdown in HCFs. One of the significantly downregulated genes was *NRAS* (Figure 6A), which regulates mitosis and cell proliferation through the Ras (Rat sarcoma or small GTPase)-Raf (Rapidly Accelerated Fibrosarcoma kinase)-MEK (trametinib [Mekinist], cobimetinib [Cotellic], and binimetinib [Mektovi])-ERK signaling pathway.³⁹ Knockdown of CDCP1 also led to an increase in the expression of *CCNG1* (Figure 6A), which encodes a cell cyclin protein that is associated with G2/M phase arrest and the inhibition of cell proliferation.⁴⁰ Interestingly, *PDGFB* expression was also significantly decreased in HCFs after CDCP1 knockdown (Figure 6A), a result suggesting a positive feedback loop between CDCP1 and PDGF signaling since PDGF-BB treatment induces CDCP1 expression in HCFs (Figure 4). These RNA-seq results provided more evidence that CDCP1 plays an important role in PDGF-BB-induced HCF proliferation.

The RNA-seq data also made it possible to compare the expression level of genes of interest in HCFs, for example, baseline expression of *CDCP1* is relatively low compared with that of genes involved in ECM (extracellular matrix) deposition (Figure 6C). *CDCP1* knockdown did not affect expression of those ECM genes, as well as TGF- β signaling genes, including *TGFB1*, *TGFBR1*, and *TGFBR2* (Figure 6C), results that support the conclusion that CDCP1 has no direct impact on TGF- β 1 signaling (Figure 5). *PDGFRA* expression was higher than *PDGFRB*, which was minimally expressed in HCFs (Figure 6C), suggesting a dominant role of PDGFR α

Figure 5 Continued. with or without CDCP1 OE and with or without half an hour of TGF- β 1 treatment (10 ng/mL). **F**, Relative protein level quantified from 3 independent samples by Western blot assays as represented in **E**. Protein levels were normalized to GAPDH level and then to vehicle and empty vector control (EV Ctrl) sample. Error bars represent SDs of triplicate assays. *P* values were calculated by ordinary 1-way ANOVA with Tukey multiple comparisons test. **G**, Immunofluorescence (IF) staining of α -SMA and VIM (vimentin) in HCFs transfected with empty vector (EV Ctrl) and CDCP1 cDNA plasmid (CDCP1 OE) and TGF- β 1 treatment (10 ng/mL) at 0.5, 24, and 72 hours. Scale bars represent 100 μ m. **H**, Percentage of α -SMA+ cells based on the IF staining as represented in **G**. Total cell number was counted by 4',6-diamidino-2-phenylindole (DAPI) staining. For each condition, α -SMA+ cells were counted from 10 different fields in triplicate independent wells. *P* values were calculated by multiple unpaired *t* tests. **I**, CDCP1 function in cardiac fibroblasts. PDGF-BB (platelet-derived growth factor subunit B homodimer) stimulates cardiac fibroblast proliferation, as well as upregulation of the maker of proliferation Ki-67 (MKI67). Expression of CDCP1 was upregulated in PDGF-BB-stimulated proliferating cardiac fibroblasts. TGF- β 1 stimulates cardiac fibroblast-to-myofibroblast transdifferentiation, which, meanwhile, stops cardiac fibroblast proliferation, as indicated by downregulation of MKI67 and upregulation of α -SMA (also known as cell growth-inhibiting gene 46 protein) in cardiac myofibroblasts. Extracellular matrix genes, including COL1A1 and FN-1, were upregulated in myofibroblasts. CDCP1 knockdown (KD) inhibits cardiac fibroblast cell proliferation, which could lead to less transdifferentiated myofibroblasts.

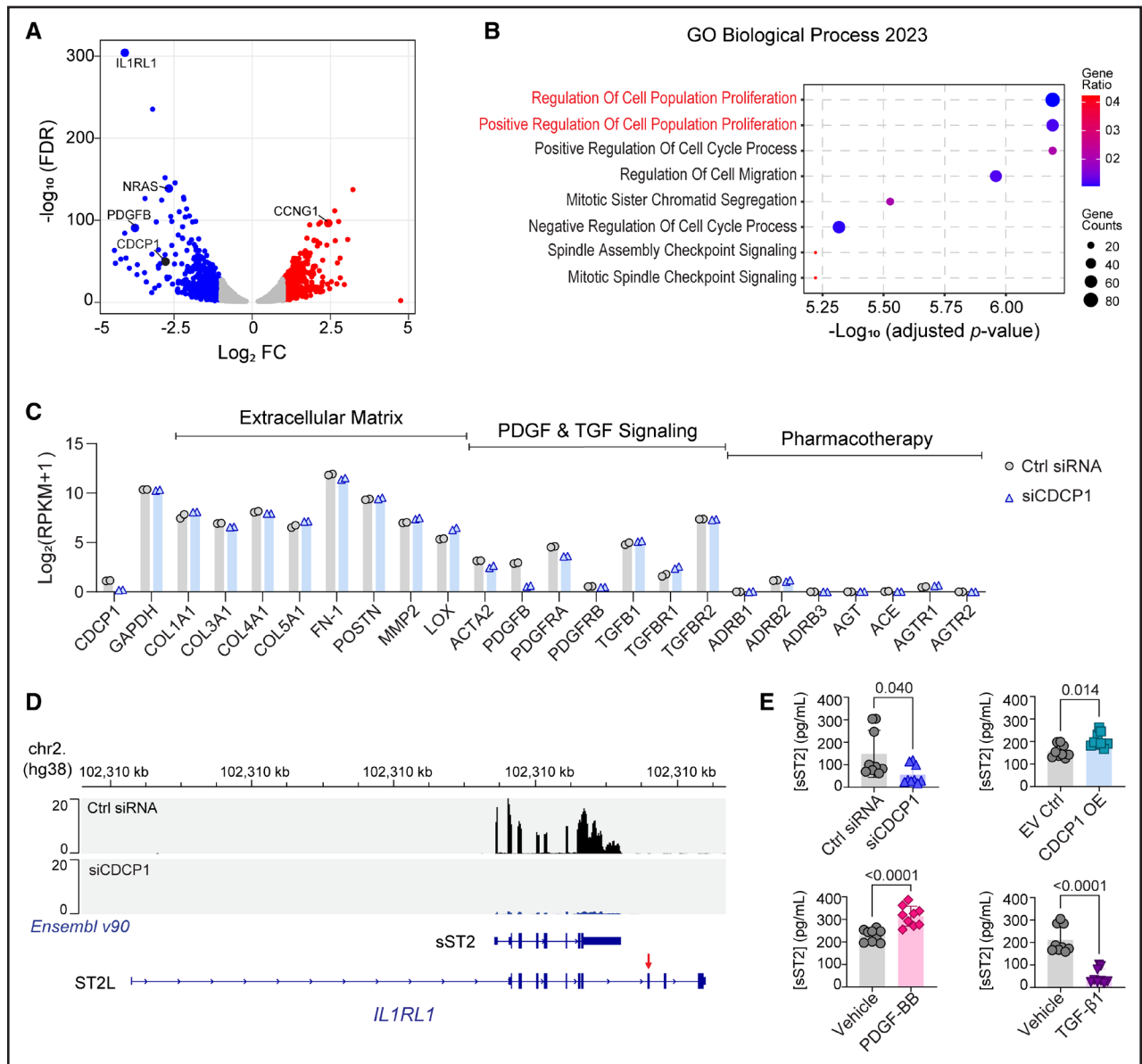


Figure 6. Transcriptome profiling of CDCP1 (CUB domain containing protein 1) knockdown (KD) in human cardiac fibroblasts (HCFs).

A, Volcano plot for RNA sequencing (RNA-seq) identified differentially expressed genes (DEGs) in HCFs after CDCP1 KD. The x axis is \log_2 fold change (FC) in RNA level when comparing the HCFs transfected with CDCP1 siRNAs (siCDCP1) to the nontarget control siRNAs (Ctrl siRNA). The y axis is $-\log_{10}$ false discovery rate (FDR) calculated from duplicates. Two biological replicate RNA samples from each experiment groups were sequenced. Each dot represents a gene quantified by the RNA-seq. **B**, Top pathways enriched by DEGs after CDCP1 KD (FC, >2.0 ; FDR, <0.05) in the gene ontology (GO) enrichment analysis of biological process. The P value for pathway enrichment was computed from the Fisher exact test and adjusted by using the Benjamini-Hochberg method for correction for multiple hypotheses testing. **C**, Gene expression level in HCFs quantified by RNA-seq. RNA level of CDCP1, GAPDH, and gene function in extracellular matrix, PDGF (platelet-derived growth factor), and TGF (transforming growth factor transforming growth factor beta) signaling, and genes involved in the mechanism of actions of standard dilated cardiomyopathy (DCM) pharmacotherapy were plotted. **D**, RNA-seq reads mapping to the *IL1RL1* gene in HCFs. From **top to bottom** are physical position of the *IL1RL1* gene on chromosome 2 based on the human genome assembly hg38; RNA-seq reads mapped to the *IL1RL1* gene in HCFs transfected with nontargeting control (Ctrl siRNA) and CDCP1 siRNA (siCDCP1); 2 *Ensembl* (v90) annotated *IL1RL1* transcript variants that encode soluble ST2 (suppression of tumorigenicity-2; sST2) and ST2 long transcript or trans-membrane receptor (ST2L). The red arrow indicates the exon that encodes the transmembrane domain of ST2L. RNA-seq reads mapped to the *IL1RL1* exons that encode sST2, and those RNA-seq reads are significantly less in CDCP1 KD (siCDCP1) sample. **E**, sST2 protein levels in HCF culture media quantified by the ELISA assay. HCFs were transfected with siCDCP1 for KD (**upper left**), CDCP1 cDNA plasmid for OE (**upper right**), and treated with 20 ng/mL of PDGF-BB (PDGF subunit B homodimer; **lower left**) or 10 ng/ μ L of TGF- β 1 (**lower right**) for 48, 72, and 96 hours. For each group, 3 biological replicates were quantified at 3 time points ($n=9$). Data are presented as mean values \pm SD. The Mann-Whitney U test was used to calculate the presented P values. RPKM indicates Reads Per Kilobase of transcript, per Million mapped reads.

in PDGF-BB-stimulated HCF proliferation (Figure 4). In addition, genes that encode standard DCM drug targets such as *ADRB1*, *ACE*, and *ATGR1* were not or only minimally expressed in HCFs (Figure 6C), which explains the absence of a change in *CDCP1* expression in HCFs when exposed to standard DCM drugs (Figure S12).

Finally, the most significantly downregulated gene after *CDCP1* knockdown was *IL1RL1* (Figure 6A), which encodes both ST2 long transcript or trans-membrane receptor (ST2L) and sST2, dependent on different *IL1RL1* transcript variants (Figure 6D). Our RNA-seq data demonstrated that, in HCFs, *IL1RL1* was transcribed to the mRNA variant, which encodes sST2, for example, RNA-seq reads mapped to the *IL1RL1* transcript variant, which encodes sST2 but not ST2L (Figure 6D). This observation was validated by *CDCP1* overexpression, which resulted in a significant increase in *IL1RL1*, as well as *PDGFB* mRNA levels in HCFs after 48 hours of *CDCP1* cDNA transfection (Figure S13). A significant decrease or increase in secreted sST2 protein levels in HCF culture media was also observed after *CDCP1* knockdown or overexpression, respectively (Figure 6E, top). The sST2 level in HCF media was tightly associated with *CDCP1* expression, that is, it was significantly increased with PDGF-BB treatment (Figure 6E, lower left), which upregulates *CDCP1*, and it was significantly decreased with TGF- β 1 treatment (Figure 6E, lower right), which represses *CDCP1*. sST2 is a well-established prognostic biomarker for heart failure.^{11,12} Specifically, elevated circulating sST2 level is associated with poor prognosis and is considered to be an inducer of heart failure and collagen synthesis.¹² These results indicate that knockdown of *CDCP1*, which leads to a decrease in sST2 expression in HCFs, may have antifibrotic and protective roles in myocardial recovery. This result is also consistent with our GWAS result that the rs6773435 SNP variant allele was associated with decreased *CDCP1* expression and improved cardiac function.

DISCUSSION

DCM is a major cause of heart failure, and drug treatment response among individual patients is highly variable (Figure 1). In an attempt to discover genetic markers that might contribute to this variable response, we applied a stepwise strategy that began with a discovery GWAS for changes in LVEF in 686 patients with recent-onset DCM. That GWAS identified a top SNP, rs6673435 (G>T), mapping to the 5'-flanking region of the *CDCP1* gene on chromosome 3 (Figure 2). The rs6673435 SNP variant allele, T, was associated with improved LVEF in those patients with DCM (Table S2). We then performed in-depth functional genomic studies to demonstrate that the T allele was associated with decreased *CDCP1* transcription in HCFs (Figure 3E) and that *CDCP1* expression was required for HCF proliferation (Figure 4) but

not for fibroblast-to-myofibroblast transdifferentiation (Figure 5). Knockdown of *CDCP1* resulted in a significant downregulation of sST2 (Figure 6), elevated levels of which are associated with increased heart failure mortality and cardiac fibrosis. In summary, the application of this strategy supported the conclusion that reduced *CDCP1* expression may contribute to myocardial recovery in DCM by attenuating cardiac fibrosis.

Cardiac fibroblast migration to and proliferation at injury sites is an initial step in response to myocardial injury.³⁴⁻³⁶ This process can be stimulated by PDGFs secreted from platelets that accumulate at these injury sites. Those cardiac fibroblasts are then transdifferentiated to myofibroblasts leading to ECM deposition and cardiac fibrosis.³⁴⁻³⁶ We demonstrated that *CDCP1* knockdown represses HCF proliferation induced by PDGF-BB treatment (Figures 4 and 5). Those heart-resident proliferating fibroblasts are the major origin of cardiac myofibroblasts, which secrete ECM proteins,^{41,42} resulting in interstitial myocardial fibrosis, a histological hallmark of DCM.⁴³ Cardiac fibrosis impedes transmission of force and mechanoelectric coupling of cardiomyocytes, decreases myocardial oxygen diffusion, and impairs coronary flow reserve by perivascular fibrosis and by paracrine mechanisms that cause myocardial dysfunction.^{44,45} The presence and extent of cardiac fibrosis assessed by magnetic resonance imaging, after adjustment for LVEF and other prognostic factors, is independently and incrementally associated with cardiovascular mortality in DCM.⁴⁶ In fact, cardiac fibrosis surpasses LVEF as a prognostic marker in heart failure.¹⁰ Importantly, the extent of cardiac fibrosis, that may be reduced with decreased HCF proliferation as a result of decreased *CDCP1* expression (Figure 4), predicts the extent of myocardial recovery in DCM,^{47,48} and the absence of cardiac fibrosis is a strong and independent predictor of improvement in LVEF and left ventricular end-diastolic volumes in patients with DCM irrespective of severity of symptoms and initial LVEF.⁴⁹

Standard heart failure therapy was used in this study population (Table S1). Although current pharmacotherapy may also have a beneficial effect by inhibiting fibroblast activation and collagen deposition,^{50,51} this effect is unlikely to be mediated by its direct action on cardiac fibroblasts since those drug-targeting genes are not expressed in HCFs (Figure 6C). Unlike current pharmacotherapy, directly targeting cardiac fibroblasts by CAR (chimeric antigen receptor) T cells has improved heart function in preclinical models and can be a new therapeutic strategy.⁵² Therefore, the identification of a novel gene associated with clinical myocardial recovery in our GWAS and the demonstration of its role in cardiac fibroblast physiology, cardiac fibrosis, and HFrEF could have important implications for the development of new heart failure therapies. *CDCP1* expression in normal heart tissue (Figure S5) and in HCFs (Figure 6C)

is low. However, we have demonstrated that CDCP1 is significantly upregulated and contributes to HCF proliferation after activation of PDGF signaling, a profibrotic growth factor that promotes cardiac fibrosis.^{34–37} The PDGF-BB-stimulated HCF proliferation (Figure 4) was predominantly mediated by PDGFR α , which is more significantly expressed than PDGFR β in HCFs (Figure 6C). PDGFR α is essential for cardiac fibroblast survival,⁵³ and reduction of PDGFR α + fibroblasts in murine hearts resulted in improvement in cardiac function after injury.⁵⁴ We demonstrated that *CDCP1* knockdown reduced HCF proliferation stimulated by PDGF-BB (Figure 4), suggesting a possible role for targeting CDCP1 to modulate cardiac fibrosis and function. An important and relevant finding was that CDCP1 knockdown significantly reduced sST2 expression (Figure 6). Plasma sST2 level is a well-established prognostic biomarker for heart failure.^{11,12} HCFs express sST2 but not its transmembrane form (Figure 6D), indicating that HCFs could potentially contribute directly to plasma sST2 levels, levels that have been associated with cardiac fibrosis, adverse cardiac remodeling, and worse cardiovascular outcomes in patients with heart failure.^{11,12}

The role of CDCP1 that we have identified in HCFs and the fact that it is inducible by PDGF-BB and regulates cell proliferation (Figure 4) is consistent with its known role in cancer. CDCP1 has been found to be significantly upregulated in a variety of cancers in which it promotes cancer cell growth and metastasis.^{25–30} In addition to the fact that CDCP1 is a single-pass cytoplasm membrane glycoprotein,²⁵ those findings make CDCP1 an intriguing potential druggable target for cancer therapy.^{25–30} Several therapeutic reagents have been developed that target CDCP1 for cancer and have shown promising efficacy and toxicity tolerance in animal models.^{25,30} CDCP1 (previously named CD318) was also found to be upregulated in immune cells and other disease states^{31–33} including heart failure comorbid with inflammatory disease.³¹

Finally, we should point out the limitations of our studies, beginning with the fact that the *P* values for association of those SNPs in our GWAS did not reach the generally accepted threshold for genome-wide significance ($P \leq 5 \times 10^{-8}$; Figure 2). Validation of those associations will be required in a larger cohort when that is possible—something that has proven to be difficult for patients with recent-onset DCM. The retrospective design of our GWAS limited our ability to investigate the *CDCP1* SNP/gene function in HCFs derived from the same patient cohort. Although we demonstrated that the rs6773435 SNP affects *CDCP1* transcriptional activity in HCFs (Figure 3F), the molecular mechanism by which the transcriptional activity is affected has not been identified and requires further studies. An SNP mapping to noncoding candidate *cis*-regulatory DNA element, such as rs6773435, could affect gene transcription through

different mechanisms including SNP-dependent chromatin modification, chromatin looping, and transcription factor binding.^{55,56} We used HCFs to study *CDCP1* function because the function annotation of SNP locus supports a role for *CDCP1* in HCFs (Figure 3) and *CDCP1* has been reported to play role in pulmonary fibrosis.⁸ However, CDCP1 also can be upregulated in immune and epithelial cells. Whether CDCP1 functions in other cell types/tissues that might contribute to myocardial recovery is unknown and should be the subject of future studies. Obviously, molecular function based on cell line models is not able to provide a comprehensive view of physiological processes underlying clinical phenotypes. The generation of *Cdcp1* knockout mice is currently ongoing in our laboratory to make it possible to further pursue the observations reported here.

In summary, we performed a discovery GWAS to assess genetic determinants of change in LVEF in patients with DCM, which identified an SNP signal mapping to the 5'-flanking region of the *CDCP1* gene. Functional genomic studies demonstrated that decreased CDCP1 expression reduces HCF proliferation stimulated by PDGF signaling. Our results support the hypothesis that decreased CDCP1 expression may contribute to the recovery of heart function in patients with recent-onset DCM by attenuating cardiac fibrosis.

Affiliations

Departments of Molecular Pharmacology and Experimental Therapeutics (D.L., V.M., T.T.L.N., T.J.P., H.G., R.M.W., N.L.P.), Cardiovascular Medicine (M.W., V.M., H.V., J.S., N.L.P.), Medicine (V.M.), Psychiatry and Psychology (M.K.S.), Health Sciences Research (A.B., G.D.J.), Cardiovascular Surgery (J.D.M.), and Physiology and Biomedical Engineering (D.J.T.), Mayo Clinic, Rochester, MN. Department of Medicine, University of Pittsburgh, PA (D.M.M.). Department of Cardiovascular Medicine, Cleveland Clinic, OH (R.C.S.). Department of Cardiovascular Medicine, Mayo Clinic, Jacksonville, FL (L.T.C.). Department of Cardiovascular Research, Istituto di Ricovero e Cura a Carattere Scientifico–Istituto di Ricerche Farmacologiche Mario Negri, Milan, Italy (S.B., S.P.). Division of Cardiology, Department of Medicine, Cardiovascular Institute, University of Colorado School of Medicine, Aurora (L.M.). Cardiothoracovascular Department, Azienda Sanitaria Universitaria Giuliano Isontina, University of Trieste, Italy (M.M., G.S.). Pôle Cardio-vasculaire et Pulmonaire, University Lille, Inserm, CHU Lille, Institut Pasteur de Lille, France (F.P., P.d.G.). First Department of Internal Medicine, Cardiology and Angiology, St. Anne's University Hospital and Masaryk University, Brno, Czech Republic (J.K., A.C.). CHU Lille, Service de Cardiologie, France (P.d.G.).

Acknowledgments

The authors thank Dr Leila Jones and Svetlana Bornschlegl from the Mayo Clinic Center for Individualized Medicine for their administration and management of this project. The authors want to thank all the participants who donated their blood samples for this study and the investigative groups from all patient-recruiting sites who helped with DNA sample collection. The authors want to thank the Gene-Tissue Expression Project, the UK Biobank, and the Encyclopedia of DNA Elements Consortium for generating the data sets that have been cited in this study.

Sources of Funding

This study was supported by the Mayo Clinic Department of Cardiovascular Medicine and Center for Individualized Medicine through internal fundings. M. Wang was supported by the National Institutes of Health (NIH) T32 Training

Grant in Clinical Pharmacology (GM08685). The IMAC-2 study (Intervention in Myocarditis and Acute Cardiomyopathy-2) was funded by the NIH R01 grant (HL075038).

Disclosures

R.M. Weinshilboum is a cofounder of and stockholder in OneOme, LLC. The other authors report no conflicts.

REFERENCES

- Go AS, Mozaffarian D, Roger VL, Benjamin EJ, Berry JD, Baha MJ, Dai S, Ford ES, Fox CS, Franco S, et al; American Heart Association Statistics Committee and Stroke Statistics Subcommittee. Heart disease and stroke statistics—2014 update: a report from the American Heart Association. *Circulation*. 2014;129:e28–e292. doi: 10.1161/01.cir.0000441139.02102.80
- Rosenbaum AN, Agre KE, Pereira NL. Genetics of dilated cardiomyopathy: practical implications for heart failure management. *Nat Rev Cardiol*. 2020;17:286–297. doi: 10.1038/s41569-019-0284-0
- McMurray JJ, Packer M, Desai AS, Gong J, Lefkowitz MP, Rizkala AR, Rouleau JL, Shi VC, Solomon SD, Swedberg K, et al; PARADIGM-HF Investigators and Committees. Angiotensin-neprilysin inhibition versus enalapril in heart failure. *N Engl J Med*. 2014;371:993–1004. doi: 10.1056/NEJMoa1409077
- McNamara DM, Starling RC, Cooper LT, Boehmer JP, Mather PJ, Janosko KM, Gorcsan J 3rd, Kip KE, Dec GW; IMAC Investigators. Clinical and demographic predictors of outcomes in recent onset dilated cardiomyopathy: results of the IMAC (Intervention in Myocarditis and Acute Cardiomyopathy)-2 study. *J Am Coll Cardiol*. 2011;58:1112–1118. doi: 10.1016/j.jacc.2011.05.033
- Kramer DG, Trikalinos TA, Kent DM, Antonopoulos GV, Konstam MA, Udelson JE. Quantitative evaluation of drug or device effects on ventricular remodeling as predictors of therapeutic effects on mortality in patients with heart failure and reduced ejection fraction: a meta-analytic approach. *J Am Coll Cardiol*. 2010;56:392–406. doi: 10.1016/j.jacc.2010.05.011
- Sanseau P, Agarwal P, Barnes MR, Pastinen T, Richards JB, Cardon LR, Mooser V. Use of genome-wide association studies for drug repositioning. *Nat Biotechnol*. 2012;30:317–320. doi: 10.1038/nbt2151
- Meder B, Ruhle F, Weis T, Homuth G, Keller A, Franke J, Peil B, Lorenzo Bermejo J, Frese K, Hüge A, et al. A genome-wide association study identifies 6p21 as novel risk locus for dilated cardiomyopathy. *Eur Heart J*. 2014;35:1069–1077. doi: 10.1093/eurheartj/ehu251
- Noskovicova N, Heinzlmann K, Burgstaller G, Behr J, Eickelberg O. Cub domain-containing protein 1 negatively regulates TGF-beta signaling and myofibroblast differentiation. *Am J Physiol Lung Cell Mol Physiol*. 2018;314:L695–L707. doi: 10.1152/ajplung.00205.2017
- Iwata M, Torok-Storb B, Wayner EA, Carter WG. CDCP1 identifies a CD146 negative subset of marrow fibroblasts involved with cytokine production. *PLoS One*. 2014;9:e109304. doi: 10.1371/journal.pone.0109304
- Schelbert EB, Piehler KM, Zareba KM, Moon JC, Ugander M, Messroghli DR, Valeti US, Chang CC, Shroff SG, Diez J, et al. Myocardial fibrosis quantified by extracellular volume is associated with subsequent hospitalization for heart failure, death, or both across the spectrum of ejection fraction and heart failure stage. *J Am Heart Assoc*. 2015;4:e002613. doi: 10.1161/JAHA.115.002613
- Kakkar R, Lee RT. The IL-33/ST2 pathway: therapeutic target and novel biomarker. *Nat Rev Drug Discov*. 2008;7:827–840. doi: 10.1038/nrd2660
- Aimo A, Januzzi JL Jr, Baynes-Genis A, Vergaro G, Sciarone P, Passino C, Emdin M. Clinical and prognostic significance of sST2 in heart failure: JACC review topic of the week. *J Am Coll Cardiol*. 2019;74:2193–2203. doi: 10.1016/j.jacc.2019.08.1039
- Gupta M, Neavin D, Liu D, Biernacka J, Hall-Flavin D, Bobo WV, Frye MA, Skime M, Jenkins GD, Batzler A, et al. TSPAN5, ERICH3 and selective serotonin reuptake inhibitors in major depressive disorder: pharmacometabolics-informed pharmacogenomics. *Mol Psychiatry*. 2016;21:1717–1725. doi: 10.1038/mp.2016.6
- Liu D, Ray B, Neavin DR, Zhang J, Athreya AP, Biernacka JM, Bobo WV, Hall-Flavin DK, Skime MK, Zhu H, et al. Beta-defensin 1, aryl hydrocarbon receptor and plasma kynurenine in major depressive disorder: metabolomics-informed genomics. *Transl Psychiatry*. 2018;8:10. doi: 10.1038/s41398-017-0056-8
- Fasching PA, Liu D, Scully S, Ingle JN, Lyra PC, Rack B, Hein A, Ekici AB, Reis A, Schneeweiss A, et al. Identification of two genetic loci associated with leukopenia after chemotherapy in patients with breast cancer. *Clin Cancer Res*. 2022;28:3342–3355. doi: 10.1158/1078-0432.CCR-20-4774
- Liu D, Zhuang Y, Zhang L, Gao H, Neavin D, Carrillo-Roa T, Wang Y, Yu J, Qin S, Kim DC, et al. ERICH3: vesicular association and antidepressant treatment response. *Mol Psychiatry*. 2021;26:2415–2428. doi: 10.1038/s41380-020-00940-y
- de Groote P, Helbecque N, Lamblin N, Hermant X, Amouyel P, Bauters C, Dallongeville J. Beta-adrenergic receptor blockade and the angiotensin-converting enzyme deletion polymorphism in patients with chronic heart failure. *Eur J Heart Fail*. 2004;6:17–21. doi: 10.1016/j.ejheart.2003.09.006
- Lemesle G, Maury F, Beseme O, Ovarit L, Amouyel P, Lamblin N, de Groote P, Bauters C, Pinet F. Multimarker proteomic profiling for the prediction of cardiovascular mortality in patients with chronic heart failure. *PLoS One*. 2015;10:e0119265. doi: 10.1371/journal.pone.0119265
- The GTEx Consortium. The Genotype-Tissue Expression (GTEx) project. *Nat Genet*. 2013;45:580–585. doi: 10.1038/ng.2653
- Encode Project Consortium. An integrated encyclopedia of DNA elements in the human genome. *Nature*. 2012;489:57–74. doi: 10.1038/nature11247
- Robinson JT, Thorvaldsdottir H, Winckler W, Guttman M, Lander ES, Getz G, Mesirov JP. Integrative genomics viewer. *Nat Biotechnol*. 2011;29:24–26. doi: 10.1038/nbt.1754
- Schneider BP, Shen F, Gardner L, Radovich M, Li L, Miller KD, Jiang G, Lai D, O'Neill A, Sparano JA, et al. Genome-wide association study for anthracycline-induced congestive heart failure. *Clin Cancer Res*. 2017;23:43–51. doi: 10.1158/1078-0432.CCR-16-0908
- Smith NL, Felix JF, Morrison AC, Demissie S, Glazer NL, Loehr LR, Cupples LA, Dehghan A, Lumley T, Rosamond WD, et al. Association of genome-wide variation with the risk of incident heart failure in adults of European and African ancestry: a prospective meta-analysis from the cohorts for heart and aging research in genomic epidemiology (CHARGE) consortium. *Circ Cardiovasc Genet*. 2010;3:256–266. doi: 10.1161/CIRCGENETICS.109.895763
- Li W, Notani D, Rosenfeld MG. Enhancers as non-coding RNA transcription units: recent insights and future perspectives. *Nat Rev Genet*. 2016;17:207–223. doi: 10.1038/nrg.2016.4
- Khan T, Kryza T, Lyons NJ, He Y, Hooper JD. The CDCP1 signaling hub: a target for cancer detection and therapeutic intervention. *Cancer Res*. 2021;81:2259–2269. doi: 10.1158/0008-5472.CAN-20-2978
- Alajati A, D'Ambrosio M, Troiani M, Mosole S, Pellegrini L, Chen J, Revandkar A, Bolis M, Theurillat JP, Guccini I, et al. CDCP1 overexpression drives prostate cancer progression and can be targeted in vivo. *J Clin Invest*. 2020;130:2435–2450. doi: 10.1172/JCI131133
- Forte L, Turdo F, Ghirelli C, Aiello P, Casalini P, Iorio MV, D'ippolito E, Gasparini P, Agresti R, Belmonte B, et al. The PDGFRbeta/ERK1/2 pathway regulates CDCP1 expression in triple-negative breast cancer. *BMC Cancer*. 2018;18:586. doi: 10.1186/s12885-018-4500-9
- Karachaliou N, Chaib I, Cardona AF, Berenguer J, Bracht JWP, Yang J, Cai X, Wang Z, Hu C, Drodzowskyj A, et al. Common co-activation of AXL and CDCP1 in EGFR-mutation-positive non-smallcell lung cancer associated with poor prognosis. *EBioMedicine*. 2018;29:112–127. doi: 10.1016/j.ebiom.2018.02.001
- Liu H, Ong SE, Badu-Nkansah K, Schindler J, White FM, Hynes RO. CUB-domain-containing protein 1 (CDCP1) activates Src to promote melanoma metastasis. *Proc Natl Acad Sci USA*. 2011;108:1379–1384. doi: 10.1073/pnas.1017228108
- Lim SA, Zhou J, Martinko AJ, Wang YH, Filippova EV, Steri V, Wang D, Remesh SG, Liu J, Hann B, et al. Targeting a proteolytic neoepitope on CUB domain containing protein 1 (CDCP1) for RAS-driven cancers. *J Clin Invest*. 2022;132:e154604. doi: 10.1172/JCI154604
- Ahlers MJ, Lowery BD, Farber-Eger E, Wang TJ, Bradham W, Ormseth MJ, Chung CP, Stein CM, Gupta DK. Heart failure risk associated with rheumatoid arthritis-related chronic inflammation. *J Am Heart Assoc*. 2020;9:e014661. doi: 10.1161/JAHA.119.014661
- Gruber CN, Patel RS, Trachtman R, Lepow L, Amanat F, Krammer F, Wilson KM, Onel K, Geanon D, Tuballes K, et al. Mapping systemic inflammation and antibody responses in multisystem inflammatory syndrome in children (MIS-C). *Cell*. 2020;183:982–995.e14. doi: 10.1016/j.cell.2020.09.034
- Lun Y, Borjini N, Miura NN, Ohno N, Singer NG, Lin F. CDCP1 on dendritic cells contributes to the development of a model of Kawasaki disease. *J Immunol*. 2021;206:2819–2827. doi: 10.4049/jimmunol.2001406

34. Travers JG, Kamal FA, Robbins J, Yutzey KE, Blaxall BC. Cardiac fibrosis: the fibroblast awakens. *Circ Res.* 2016;118:1021–1040. doi: 10.1161/CIRCRESAHA.115.306565
35. Frangogiannis NG. Cardiac fibrosis. *Cardiovasc Res.* 2021;117:1450–1488. doi: 10.1093/cvr/cvaa324
36. Schreiber F, Anslinger TM, Kramann R. Fibrosis in pathology of heart and kidney: from deep RNA-sequencing to novel molecular targets. *Circ Res.* 2023;132:1013–1033. doi: 10.1161/CIRCRESAHA.122.321761
37. Gallini R, Lindblom P, Bondjers C, Betsholtz C, Andrae J. PDGF-A and PDGF-B induces cardiac fibrosis in transgenic mice. *Exp Cell Res.* 2016;349:282–290. doi: 10.1016/j.yexcr.2016.10.022
38. Manning BD, Toker A. AKT/PKB signaling: navigating the network. *Cell.* 2017;169:381–405. doi: 10.1016/j.cell.2017.04.001
39. McCubrey JA, Steelman LS, Chappell WH, Abrams SL, Wong EW, Chang F, Lehmann B, Terrian DM, Milella M, Tafuri A, et al. Roles of the Raf/MEK/ERK pathway in cell growth, malignant transformation and drug resistance. *Biochim Biophys Acta.* 2007;1773:1263–1284. doi: 10.1016/j.bbamcr.2006.10.001
40. Kimura SH, Ikawa M, Ito A, Okabe M, Nojima H. Cyclin G1 is involved in G2/M arrest in response to DNA damage and in growth control after damage recovery. *Oncogene.* 2001;20:3290–3300. doi: 10.1038/sj.onc.1204270
41. Kanisicak O, Khalil H, Ivey MJ, Karch J, Maliken BD, Correll RN, Brody MJ, Suh-Chin JL, Aronow BJ, Tallquist MD, et al. Genetic lineage tracing defines myofibroblast origin and function in the injured heart. *Nat Commun.* 2016;7:12260. doi: 10.1038/ncomms12260
42. Moore-Morris T, Guimaraes-Camboa N, Banerjee I, Zambon AC, Kisseleva T, Velayoudon A, Stallcup WB, Gu Y, Dalton ND, Cedenilla M, et al. Resident fibroblast lineages mediate pressure overload-induced cardiac fibrosis. *J Clin Invest.* 2014;124:2921–2934. doi: 10.1172/JCI74783
43. González A, Schelbert EB, Díez J, Butler J. Myocardial interstitial fibrosis in heart failure: biological and translational perspectives. *J Am Coll Cardiol.* 2018;71:1696–1706. doi: 10.1016/j.jacc.2018.02.021
44. Dai Z, Aoki T, Fukumoto Y, Shimokawa H. Coronary perivascular fibrosis is associated with impairment of coronary blood flow in patients with non-ischemic heart failure. *J Cardiol.* 2012;60:416–421. doi: 10.1016/j.jjcc.2012.06.009
45. Villari B, Campbell SE, Hess OM, Mall G, Vassalli G, Weber KT, Krայenbuehl HP. Influence of collagen network on left ventricular systolic and diastolic function in aortic valve disease. *J Am Coll Cardiol.* 1993;22:1477–1484. doi: 10.1016/0735-1097(93)90560-n
46. Gulati A, Jabbar A, Ismail TF, Guha K, Khwaja J, Raza S, Morarji K, Brown TD, Ismail NA, Dweck MR, et al. Association of fibrosis with mortality and sudden cardiac death in patients with nonischemic dilated cardiomyopathy. *JAMA.* 2013;309:896–908. doi: 10.1001/jama.2013.1363
47. Azevedo CF, Nigri M, Higuchi ML, Pomerantzeff PM, Spina GS, Sampaio RO, Tarasoutchi F, Grinberg M, Rochitte CE. Prognostic significance of myocardial fibrosis quantification by histopathology and magnetic resonance imaging in patients with severe aortic valve disease. *J Am Coll Cardiol.* 2010;56:278–287. doi: 10.1016/j.jacc.2009.12.074
48. Yamada T, Fukunami M, Ohmori M, Iwakura K, Kumagai K, Kondoh N, Minamino T, Tsujimura E, Nagareda T, Kotoh K. Which subgroup of patients with dilated cardiomyopathy would benefit from long-term beta-blocker therapy? A histologic viewpoint. *J Am Coll Cardiol.* 1993;21:628–633. doi: 10.1016/0735-1097(93)90094-h
49. Masci PG, Schuurman R, Andrea B, Ripoli A, Coceani M, Chiappino S, Todiere G, Srebot V, Passino C, Aquaro GD, et al. Myocardial fibrosis as a key determinant of left ventricular remodeling in idiopathic dilated cardiomyopathy: a contrast-enhanced cardiovascular magnetic study. *Circ Cardiovasc Imaging.* 2013;6:790–799. doi: 10.1161/CIRCIMAGING.113.000438
50. De Mello WC, Specht P. Chronic blockade of angiotensin II AT1-receptors increased cell-to-cell communication, reduced fibrosis and improved impulse propagation in the failing heart. *J Renin Angiotensin Aldosterone Syst.* 2006;7:201–205. doi: 10.3317/jraas.2006.038
51. Zannad F, Alla F, Douset B, Perez A, Pitt B. Limitation of excessive extracellular matrix turnover may contribute to survival benefit of spironolactone therapy in patients with congestive heart failure: insights from the Randomized Aldactone Evaluation Study (RALES). Rales investigators. *Circulation.* 2000;102:2700–2706. doi: 10.1161/01.cir.102.22.2700
52. Aghajanian H, Kimura T, Rurik JG, Hancock AS, Leibowitz MS, Li L, Scholler J, Monslow J, Lo A, Han W, et al. Targeting cardiac fibrosis with engineered T cells. *Nature.* 2019;573:430–433. doi: 10.1038/s41586-019-1546-z
53. Ivey MJ, Kuwabara JT, Riggsbee KL, Tallquist MD. Platelet-derived growth factor receptor- α is essential for cardiac fibroblast survival. *Am J Physiol Heart Circ Physiol.* 2019;317:H330–H344. doi: 10.1152/ajpheart.00054.2019
54. Kuwabara JT, Hara A, Bhutada S, Gojanovich GS, Chen J, Hokutan K, Shettigar V, Lee AY, DeAngelo LP, Heckl JR, et al. Consequences of PDGFR α (+) fibroblast reduction in adult murine hearts. *Elife.* 2022;11:e69854. doi: 10.7554/eLife.69854
55. Nguyen TTL, Gao H, Liu D, Philips TJ, Ye Z, Lee JH, Shi GX, Copenhaver K, Zhang L, Wei L, et al. Glucocorticoids unmask silent non-coding genetic risk variants for common diseases. *Nucleic Acids Res.* 2022;50:11635–11653. doi: 10.1093/nar/gkac1045
56. Liu D, Nguyen TTL, Gao H, Huang H, Kim DC, Sharp B, Ye Z, Lee JH, Coombes BJ, Ordog T, et al. TCF7L2 lncRNA: a link between bipolar disorder and body mass index through glucocorticoid signaling. *Mol Psychiatry.* 2021;26:7454–7464. doi: 10.1038/s41380-021-01274-z
57. McCarthy S, Das S, Kretzschmar W, Delaneau O, Wood AR, Teumer A, Kang HM, Fuchsberger C, Danecek P, Sharp K, et al. Haplotype Reference Consortium. A reference panel of 64,976 haplotypes for genotype imputation. *Nat Genet.* 2016;48:1279–1283. doi: 10.1038/ng.3643
58. Das S, Forer L, Schonherr S, Sidore C, Locke AE, Kwong A, Vrieze SI, Chew EY, Levy S, McGue M, et al. Next-generation genotype imputation service and methods. *Nat Genet.* 2016;48:1284–1287. doi: 10.1038/ng.3656
59. Genomes Project C, Auton A, Brooks LD, Durbin RM, Garrison EP, Kang HM, Korbel JO, Marchini JL, McCarthy S, McVean GA, et al. A global reference for human genetic variation. *Nature.* 2015;526:68–74. doi: 10.1038/nature15393